

Io-Jupiter decametric arcs observed by Juno/Waves compared to ExPRES simulations

C.K. Louis, L. Lamy, P. Zarka, B. Cecconi, M. Imai, W S Kurth, G. Hospodarsky, S.L.G. Hess, X. Bonnin, S Bolton, et al.

▶ **To cite this version:**

C.K. Louis, L. Lamy, P. Zarka, B. Cecconi, M. Imai, et al.. Io-Jupiter decametric arcs observed by Juno/Waves compared to ExPRES simulations. Geophysical Research Letters, 2017, 44 (18), pp.9225-9232. 10.1002/2017GL073036 . hal-01599674

HAL Id: hal-01599674

https://hal.sorbonne-universite.fr/hal-01599674

Submitted on 2 Oct 2017

HAL is a multi-disciplinary open access archive for the deposit and dissemination of scientific research documents, whether they are published or not. The documents may come from teaching and research institutions in France or abroad, or from public or private research centers.

L'archive ouverte pluridisciplinaire **HAL**, est destinée au dépôt et à la diffusion de documents scientifiques de niveau recherche, publiés ou non, émanant des établissements d'enseignement et de recherche français ou étrangers, des laboratoires publics ou privés.

AGU PUBLICATIONS

Geophysical Research Letters

RESEARCH LETTER
10.1002/2017GL073036

Special Section:
Early Results: Juno at Jupiter

Io-Jupiter decametric arcs observed by Juno/Waves compared to ExPRES simulations

C. K. Louis[1,2], L. Lamy[1,2], P. Zarka[1,2], B. Cecconi[1,2], M. Imai[3], W. S. Kurth[3], G. Hospodarsky[3], S. L. G. Hess[4], X. Bonnin[1], S. Bolton[5], J. E. P. Connerney[6], and S. M. Levin[7]

[1]LESIA, Observatoire de Paris, PSL Research University, CNRS, Sorbonne Universités, UPMC Univ. Paris 06, Univ. Paris Diderot, Sorbonne Paris Cité, Meudon, France, [2]Station de Radioastronomie de Nançay (SRN), Observatoire de Paris, CNRS USN, PSL Research University, Université d'Orléans, Nançay, France, [3]Department of Physics and Astronomy, University of Iowa, Iowa City, Iowa, USA, [4]Department of Space Environment, ONERA, Toulouse, France, [5]Space Science Department, Southwest Research Institute, San Antonio, Texas, USA, [6]NASA Goddard Space Flight Center, Greenbelt, Maryland, USA, [7]Jet Propulsion Laboratory, California Institute of Technology, Pasadena, California, USA

Key Points:
- First Juno/Waves observations compared to ExPRES simulations of Jupiter-Io decametric emission
- Near equator ExPRES simulations show that most of the arcs observed in the time-frequency plane by Juno, Wind, and Nançay are due to Io
- The simulations and observations of Io arcs are in good agreement when the modeled radio beaming angle $\theta = (\mathbf{k},\mathbf{B}) \geq 70° \pm 5°$

Supporting Information:
- Supporting Information S1

Correspondence to:
C. K. Louis,
corentin.louis@obspm.fr

Citation:
Louis, C. K., et al. (2017), Io-Jupiter decametric arcs observed by Juno/Waves compared to ExPRES simulations, *Geophys. Res. Lett.*, *44*, doi:10.1002/2017GL073036.

Received 10 FEB 2017
Accepted 16 MAR 2017

©2017. American Geophysical Union. All Rights Reserved.

Abstract We compare observations from the Juno/Waves radio experiment with simulations of radio «arcs» in the time-frequency plane resulting from the Io-Jupiter interaction, performed with the ExPRES code. We identify the hemisphere of origin of the observed arcs directly from simulations and confirm this identification through comparison with Juno, Nançay, and Wind observations. The occurrence and shape of observed arcs are well modeled, at low latitudes with their usual shapes as seen from Earth, as well as at high latitudes with longer, bowl-shaped, arcs observed for the first time. Predicted emission is actually observed only when the radio beaming angle $\theta = (\mathbf{k},\mathbf{B}) \geq 70° \pm 5°$, providing new constraints on the generation of the decameter emission by the Cyclotron Maser Instability. Further improvements of ExPRES are outlined, which will then be applied to Juno and Earth-based observations of radio emissions induced by other Galilean satellites or associated to the main auroral oval.

1. Introduction

The Juno spacecraft, in Jupiter orbit since 4 July 2016, performs observations of Jupiter radio emissions up to 40.5 MHz with the Waves experiment. The Waves data used in this paper are recorded continuously at low time-frequency (t-f) resolutions acquired in "survey" mode. This mode sweeps the 3.5–40.5 MHz range with a channel spacing of 1 MHz, every 1 s, 10 s, or 30 s.

In the decametric (DAM) wavelength range, Jupiter's radio emission is structured in the form of discrete arcs in the t-f plane, labeled "A" when the radio source is located in the north-right of Jupiter, "B" in the north-left, "C" in the south-right, and "D" in the south-left, as seen from the observer [*Carr et al.*, 1983; *Marques et al.*, 2017, and references therein]. These radio emissions are produced via the Cyclotron Maser Instability (CMI) by electrons with keV (possibly up to 10 s of keV) typical energy, gained through acceleration along magnetic field lines above the auroral regions or along magnetic flux tubes connecting Galilean satellites to Jupiter, mainly Io, but also Ganymede and Europa [*Zarka*, 1998, 2004; *Louis et al.*, 2017]. Radio emissions are produced at the local electron cyclotron frequency along these field lines ($f \sim f_{ce}$). At the footprints of these field lines, bright UV auroral emissions are generated by collisions of part of these electrons with Jupiter's upper neutral atmosphere (main oval, satellite footprint spots) [*Bagenal et al.*, 2014, and references therein].

The simulation code ExPRES [*Hess et al.*, 2008a] was created to predict arc shapes in the t-f plane recorded by any arbitrary selected observer, from the computed visibility of CMI emission from (a set of) point sources along a magnetic field line. This visibility depends in particular of the radio beaming angle, i.e., the aperture angle $\theta = (\mathbf{B},\mathbf{k})$ between the magnetic field vector at the source and the emitted wave vector. This angle is computed in a self-consistent way (ignoring refraction) in the frame of the CMI theory based on the choice of the electron distribution that drives the emission: loss cone distribution produces oblique emission with variable $\theta(f)$, whereas ring/shell distribution produces perpendicular emission ($\theta \sim 90°$) at all frequencies [*Hess et al.*, 2008a]. Such simulations have been employed to study radio emissions of Jupiter [*Hess et al.*, 2008a; *Cecconi et al.*, 2012], Saturn [*Lamy et al.*, 2008, 2013], and exoplanets [*Hess and Zarka*, 2011]. In the case of Jupiter, the first comparisons between simulations and observations of Io-DAM arcs favor oblique emission

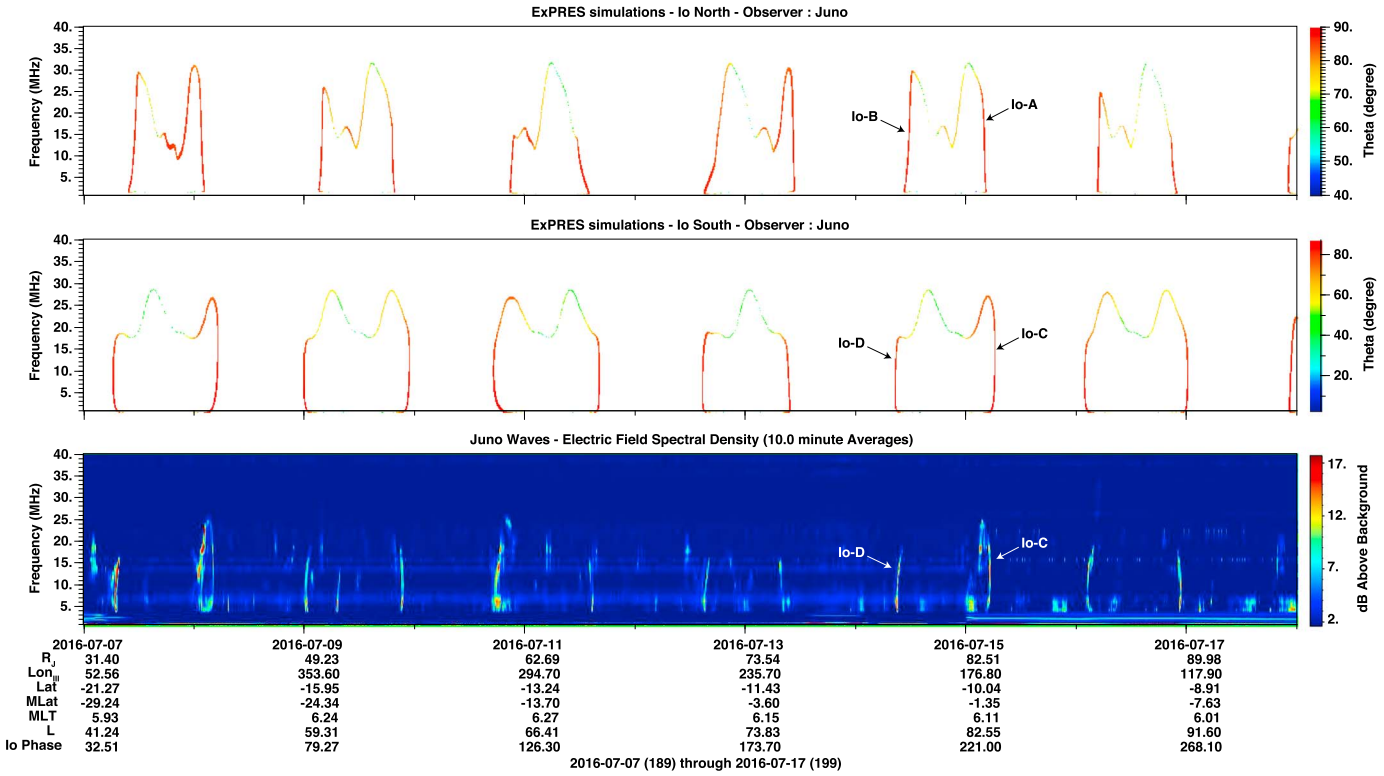


Figure 1. Juno/Waves observations (bottom panel) during 11 days after insertion into orbit, from latitudes between −30° and +1°, compared to ExPRES simulations of Io-DAM arcs from the (middle panel) southern and (top panel) northern AFT footprints as seen from Juno. The color scale of simulation panels represents the value of the radio beaming angle $\theta = (\mathbf{k},\mathbf{B})$ at the source. The scales below the plots provide the distance (R_J), system III longitude and latitude, magnetic latitude and local time, L-shell, and Io phase (from superior conjunction) of the Juno spacecraft. Examples of arcs corresponding to the "A," "B," "C," and "D" nomenclature are indicated.

[*Hess et al.*, 2008a] in spite of the fact that perpendicular emission should have larger growth rates [*Hess et al.*, 2008b]. A possible explanation for the emission produced to escape from the source region was proposed by *Mottez et al.* [2010]. Another possibility is that perpendicular emission is refracted in/near the source to emerge at oblique angles, as found for the terrestrial kilometric radiation [*Mutel et al.*, 2008], and is suspected for Saturn's kilometric radiation [*Lamy et al.*, 2011]. When simulating satellite-induced emission with ExPRES, the assumption of a single source field line is realistic: it corresponds to the magnetic flux tube along which electrons are accelerated by the satellite interaction with the Jovian field. In the case of Io, a «lead» angle exists between this active flux tube (hereafter AFT) and the instantaneous Io flux tube that is due to slow Alfvén wave propagation in the Io plasma torus combined with Jupiter's rotation. The value of this lead angle can be approximated by a sine variation versus Io's longitude [*Hess et al.*, 2011].

In this paper, we compare ExPRES simulations of Io-Jupiter emissions with observations from the Juno/Waves experiment. Earth-based observations from the Nançay Decameter Array (NDA) and from the Waves experiment on board the Wind spacecraft help radio arc identification. The simulation and comparison methods are first presented (in section 2), followed by their application to the Juno data (section 3), and then the results are discussed and perspectives are drawn (section 4).

2. Methods

Figure 1 (bottom) shows 11 days of Juno/Waves survey mode data in the 1–40 MHz range where many radio arcs are visible.

We have produced ExPRES simulations of Io-Jupiter emissions as seen from the Juno spacecraft, for all existing Juno data. The simulations are based on the Jovian internal magnetic field model ISaAC (In Situ and Auroral Constraints [*Hess et al.*, 2017]), an updated version of VIPAL [*Hess et al.*, 2011] further constrained

by Europa and Ganymede UV footprints. The magnetospheric plasma density along the AFT is described by an ionosphere and a plasma torus. The ionosphere is modeled by $\rho_{iono} = \rho_0 * e^{-(r-r_0)/H}$, with a peak density $\rho_0 = 350{,}000\,cm^{-3}$ and a topside scale height $H = 1600$ km [*Hinson et al.*, 1998]. The torus is modeled by $\rho_{torus} = \rho_0 * e^{-\sqrt{\left(\sqrt{x^2+y^2}-r_0\right)^2+z^2}/H}$, with $\rho_0 = 2000\,cm^{-3}$ at the center of the torus, at $r_0 = 5.91$ Jovian radii (R_j), and a vertical scale height $H = 1\,R_j$ [*Bagenal*, 1994]. The active field line leads the instantaneous Io field line by an angle modeled as $\delta = A + B * \cos(\lambda_{Io} - 202°)$ with $A = 2.8°$ and $B = -3.5°$ in the northern hemisphere and $A = 4.3°$ and $B = 3.5°$ in the southern hemisphere [*Hess et al.*, 2011] (equations in *Hess et al.* [2011] indicate erroneously $A + B * \cos(\lambda_{Io} - 20°)$). The electron energy is set at 0.64 keV in the northern hemisphere and 3 keV in the southern one [*Hess et al.*, 2008a]. With these energies, the loss cone-driven CMI predicts hollow emission cones with beaming angles θ between ~50° (at low frequencies) and ~90° (at high frequencies) along the arcs (see Figure 1). The cone wall thickness is fixed at 1° [*Hess et al.*, 2008a; *Kaiser et al.*, 2000]. Refraction along the raypath is neglected in this study; thus, the waves propagate in a straight line from the source to the observer. The maximum emission frequency f_{ce} is taken at the auroral peak altitude (650 km above the 1 bar level) that corresponds to a typical ionospheric limit of the loss cone, where electrons are lost by collisions.

The output of these simulations are dynamic spectra (t-f plots) where nonzero values indicate the times and frequency bins where the observer can detect CMI emission, based on the predicted geometry of the emission and the position of the observer. Additionally, the predicted polarization of the emission can be displayed (right-handed from the northern magnetic hemisphere of Jupiter, left-handed from the southern one for extraordinary mode emission), as well as the predicted radio beaming angle θ for each t-f bin. We have chosen to display t-f plots of the θ angle of predicted emissions, separately from the northern and from the southern footprints of the AFT.

Ground-based decameter observations are also conducted in support to Juno observations by a number of radio observatories grouped in a Juno.Ground.Radio collaboration [*Cecconi et al.*, 2017], including the NDA [*Lamy et al.*, 2017]. In this paper, along with Juno/Waves data, we use NDA data in the range of 10–40 MHz complemented by Wind/Waves data in the range of 1–14 MHz [*Bougeret et al.*, 1995].

For this study, we have used the Autoplot software for plotting data (http://autoplot.org [*Faden et al.*, 2010]).

3. Results

Figure 1 presents ExPRES simulations of northern and southern Io-DAM, together with Juno/Waves data, for 11 days shortly after Juno's insertion in Jupiter's orbit in July 2016. The spacecraft latitude varied between 30°S and 1°N. We notice an almost one-to-one correspondence between the observed intense arcs and the modeled ones from the southern hemisphere. All southern arcs simulated by ExPRES are indeed observed, and simulated shapes match the observations quite well, within a few hours in time and a few MHz in frequency. Most of the intense arcs observed during this 11 day continuous interval can thus be attributed to southern Io-Jupiter emission, which is consistent with the spacecraft location in the southern hemisphere.

The predicted southern emission is actually observed only when $\theta \geq 70° \pm 5°$ (red-orange color), matching frequencies generally lower than 20–25 MHz. This may be because the emission is less intense for $\theta < 70°$, in which case it may appear after deeper processing of the Juno/Waves data. However, the emission can also be less intense or absent for $\theta < 70°$. Our simulations predict t-f bins where oblique emission (produced by loss cone driven CMI) should be observed, but they do not guarantee that the emission is indeed produced at every frequency along the AFT. This depends on the presence of unstable electron distributions, for which in situ Juno/JADE (Jovian Auroral Distributions Experiment) [*McComas et al.*, 2013] measurements will be crucial. Another possibility is that emission displays apparent values of θ which significantly differ from those simulated, for instance with $\theta = 90°$ (by ring/shell-driven CMI) and refracted to an apparent beaming $\theta \sim 70°$ as observed far from the source. Measurements at various distances from the source and in situ Juno/Waves measurements will allow us to settle these questions.

The fast motion of Juno along its orbit and the high-latitude exploration result in shapes of observed arcs never seen previously, such as the nearly closed t-f loops at the beginning of 8 and 15 July 2016, which are identified as Io-Jupiter emissions and well represented by the simulations. For instance, on 8 July 2016

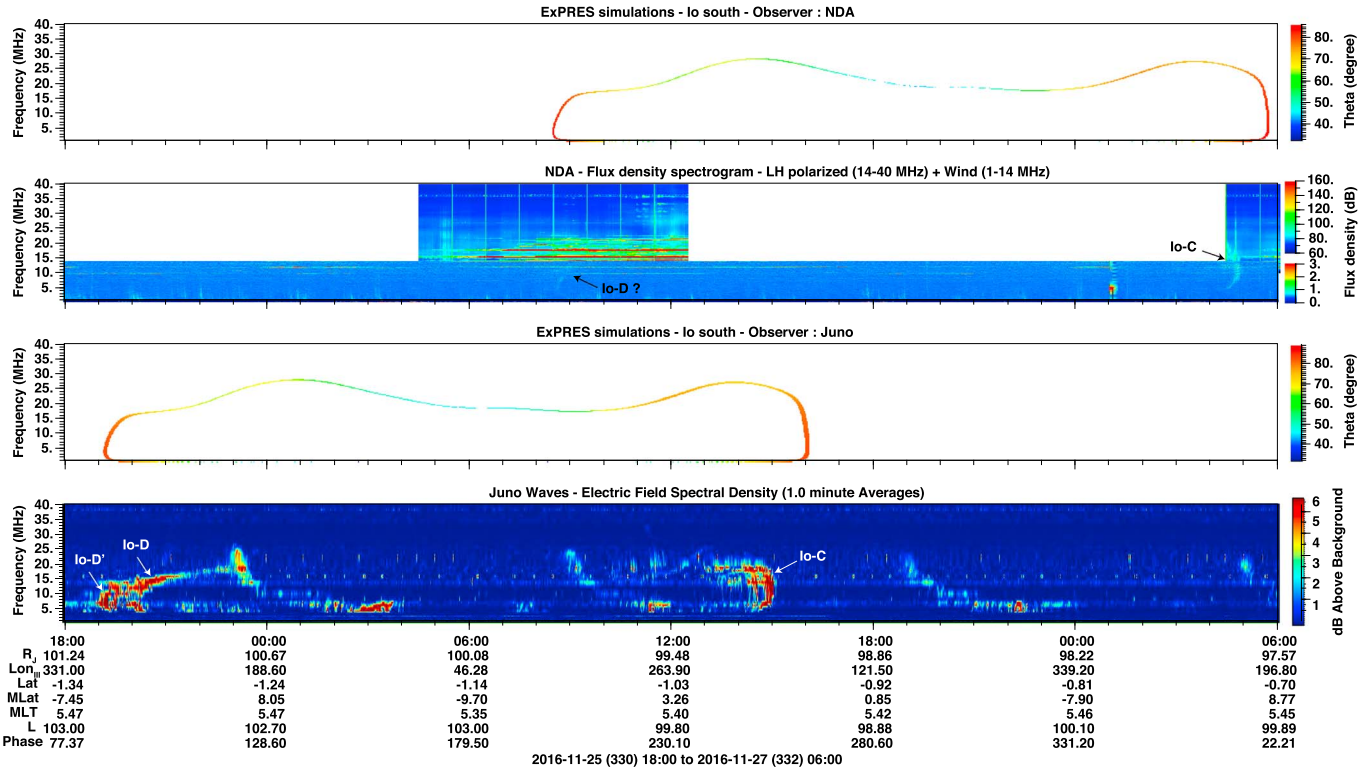


Figure 2. (bottom row) Similar to Figure 1, but for a duration of 36 h in-between 25 and 27 November 2016. In addition, (top rows) simultaneous observations from the NDA and Wind spacecraft and corresponding simulations for an Earth-based observer are shown. The Io arc observed by the NDA on 27 November 2016 at ~04:30 has dominant left-hand circular polarization. Two arcs are observed by Wind, an Io-D on 26 November 2016 at ~08:30 (very weak) and an Io-C on 27 November 2016 at ~04:30 (simultaneously with NDA).

the magnetic latitude λ_{mag} varied from $-10°$ to $-27°$ between 01:00 and 04:30. By contrast, the slower geometrical variations that affect Earth-based observations result in Io-DAM arcs generally observed as opening (so-called vertex-early) or closing (vertex-late) parentheses [e.g., *Marques et al.*, 2017, and references therein].

Northern arcs predicted by ExPRES are essentially not observed, although weaker parts of arcs may become visible after further data processing. This suggests that ExPRES simulations predict correctly the emissions originating from the hemisphere of the observer. The visibility of emission radiated from the other hemisphere is likely to be affected (or cancelled) by two main effects: (i) in/near source refraction (neglected here) that modifies the apparent θ for the emission coming from the observer's hemisphere and may cause the emission from the other hemisphere to be refracted away and result in lower apparent theta (refraction far from the source, e.g., in the Io torus, should not affect the highest frequency part of the emission); (ii) ExPRES assumes no azimuthal variation of the radio beaming angle around the magnetic field vector in the source yet, but the real beaming pattern is likely oblate, with a reduced value of θ toward the equator [*Galopeau and Boudjada*, 2016] (i.e., toward the hemisphere opposed to the source), making it not observable.

Figure 2 shows a 1.5 day interval of Juno observations and corresponding ExPRES simulations (bottom rows), for which simultaneous observations by the NDA (with circular polarization measurement) and Wind/Waves were available. They are displayed on the same panel, with corresponding ExPRES simulations above (top rows).

This close-in-view of 36 h confirms the good matching of simulations and observations of Io-DAM but shows an ~1 h discrepancy in the time of occurrence of the arcs. Such shifts in the time occurrence of the simulated arcs are expected due to the slow motion of Io around Jupiter: at ~0.14°/min, an error of 10° in θ translates into a delay of 71 min in time. (i.e., 8.5°/h). The fact that the simulated Io-D arc is ~1 h before the observed one, and the simulated Io-C arc ~1 h after the observed one, with an ~20 h separation between the two

observed arcs, suggests that θ was overestimated by ~10% in the simulation. This overestimation could be due to a wrong estimation of the energy of the electrons. Indeed, the variation in the time position of the arcs for values between 0.5 and 15 keV is ~2 h. An alternate possibility is that the lead angle is not well modeled by the sinusoidal model, because it depends on the plasma conditions of the Io torus, variable in time. As said previously, an error of 1 h corresponds to an error of 8.5°.

Figure 2 confirms that predicted emission is actually observed only when $\theta \geq 70°$ (red-orange color). The observed thickness of the arcs is consistent with a cone wall thickness ~1°, as in the simulation, which is equivalent to an infinitely thin cone thickness convolved by a 1° wide in longitude source region.

Another arc is observed before the main Io-D arc (labeled Io-D′). This feature is often observed for Io-B arcs but rarely for Io-D ones [*Queinnec and Zarka*, 1998; *Marques et al.*, 2017]. This can be interpreted by the multiple reflections of Alfvén waves between the Io torus and Jupiter's ionosphere that lead to multiple UV spots at AFT footprints [see, e.g., *Bonfond et al.*, 2008]. It seems also to be the case for the Io-C arc.

Figure S1 in the supporting information (zoom in the beginning of Figure 1) presents the nearly closed loops on 8 July 2016 (previously discussed, see Figure 1). The same correspondence between observations and simulations as in Figure 2 is observed, with the same ~1 h accuracy, and the same conclusions about θ and/or the lead angle can be drawn. As in Figure 2, the Io-D arc seen by Juno is multiple. The time separation of the arcs should match the longitudinal shift between multiple UV spots at AFT footprints. We should be able to confirm this with Juno by comparing Waves and UV measurements.

Comparison with NDA and Wind/Waves Earth-based observations brings additional information: the arc observed by the NDA on 27 November 2016 at ~04:30, observed simultaneously by Wind at low frequencies, has a dominant left-handed circular polarization, indicating an origin in Jupiter's southern hemisphere, which supports the conclusions drawn from Juno-ExPRES comparison. The arcs observed by Juno on 25 November 2016 at ~19:30 ± 00:30 and on 26 November 2016 at ~15:00 are observed ~13 h later by Wind for the first one and both the NDA and Wind for the second one. Juno being about at 5.4 h LT, and Earth about 12.5 h LT, the expected delay for a source moving with Io at ~8.5°/h is $(12.5–5.4) \times 15/8.5 \approx 12.5$ h, consistent with the observed ~13 h delay. This constitutes an independent proof of the Io-Jupiter origin of this arc, making unambiguous its identification by the simulation. It also shows that Io-Jupiter arcs last and have a stable shape over many hours. Taken with Figure 1, Figure 2 supports that the Io-Jupiter emission is essentially permanent.

The simulated Io-C arc occurs ~1 h after the time of its actual observation, both by Juno and by Wind + NDA. As explained previously, this may be due to an overestimation of the AFT delay (i.e., of the lead angle), an error on the magnetic field topology, or a small error on θ.

Figure 3 displays Juno/Waves data (bottom row), ExPRES simulations as seen from Juno (middle rows), and NDA data (top row) around periJove #1. Two Io-DAM arcs are unambiguously identified by comparing Juno/ExPRES data (labeled "Io"), on 25 August 2016 at ~18:00–19:00 for the northern AFT footprint (labeled "Io-B"), when Juno was in the northern hemisphere, and on 28 August 2016 at ~11:00–12:00 for the southern AFT footprint (labeled "Io-C"), when Juno was in the southern hemisphere. Two additional Io-DAM arcs with unusual shape (labeled "Io?") are tentatively identified just before (27 August 2016 at ~10:00–12:00) and just after (27 August 2016 at ~14:00–16:00) periJove#1 when Juno was at high latitudes. They are further discussed below.

All other observed emissions are likely to be associated with the main auroral oval (simulations made for other Galilean satellites showed no correspondence). One of them can be identified as an auroral emission comparing Juno and NDA data: the arc seen on 26 August 2016 at ~08:00 by Juno is detected by the NDA at ~10:30. This 2.5 h delay is consistent with the time needed for a source co-rotating with Jupiter (at a period ~10 h) to cover the ~6 h LT difference between Juno and NDA. Contrary to Io-Jupiter emission, the shape of the arc seems to have changed during this time interval (it does not reach as high frequencies). The difference in the covered frequencies may also be related to the different latitudes of the observers (Earth and Juno) and to the oblateness of the emission cone. Further ExPRES simulations based on the field lines of auroral UV hot spots seen by UVs should allow us to identify most of the individual radio arcs and constrain source field lines and radio beaming angles.

Figure S2 is a zoom of Figure 3 (bottom rows), for ~13 h around periJove #1. The high-latitude passes of Juno above both Jovian poles provide a totally new geometry of observation, in which Io-Jupiter arcs take unusual

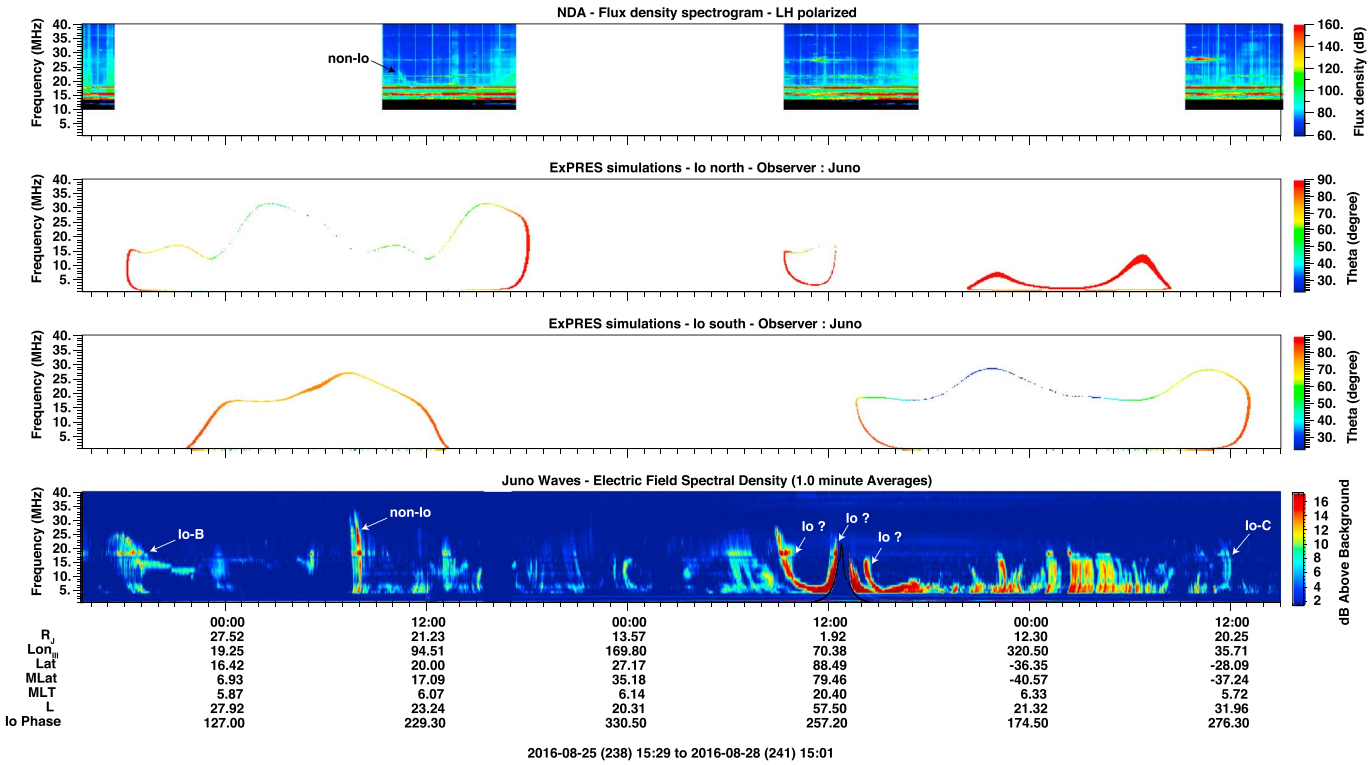


Figure 3. Juno/Waves observations (bottom row) for ~3 days around periJove #1 that occurred on 27 August 2016 at ~13:00 compared to (middle rows) ExPRES simulations of the arcs from the southern and northern AFT footprints as seen from Juno (same format as Figure 1) and to (top row) simultaneous NDA observations. Emissions identified by comparisons Juno/ExPRES or Juno/NDA are labeled.

bowl shapes in the t-f plane. Northern and southern Io-DAM arcs are tentatively identified in Juno observations based on ExPRES simulations. They are likely superimposed with auroral (non-Io) emissions. The start of the arc between 09:00 and 10:00 is certainly the high-latitude equivalent of an Io-B arc. Its end (around 12:00) seems to be superimposed with auroral emission that tangents the local f_{ce}, suggesting a radio source crossing by the spacecraft [*Kurth et al.*, 2017]. The source crossed cannot be an Io-DAM source, as the phase of Io was far from 180° at that time. Quantitative studies based on the detailed magnetic field topology will permit further investigation. JADE observations will provide electron energies and distribution functions in/near the sources [*Louarn et al.*, 2017; *Allegrini et al.*, 2017]. After periJove#1, when Juno was at high southern latitudes, a southern Io-Jupiter arc is predicted by ExPRES and falls in between two observed arcs. For the same reasons as above, we tend to identify it to the arc starting at ~14:15, while we interpret the emission just after periJove#1 as an auroral emission (again with in situ source crossings). We notice that Io-Jupiter emissions are observed from high latitudes over ranges of Io phases much broader than those determined from Earth-based near equatorial observations [*Marques et al.*, 2017]. This strongly suggests that the restricted ranges of Io phases, in which Io-Jupiter emissions are detected from Earth, mainly result from visibility effects.

4. Summary and Discussion

The dynamic spectra of Jupiter's decametric radio emissions are rich and complex, and Juno provides new observations with a unique geometry. ExPRES is a very valuable tool for simulating and interpreting such observations. The simulations allow us to identify the hemisphere of origin of the observed arcs, independent of any polarization or direction-finding measurement from the spacecraft. Most of the intense arcs observed from low latitudes are due to the Io-Jupiter interaction, and all Io-DAM arcs predicted by ExPRES from the source located in the same hemisphere as the observer are observed and identified (as tested over a continuous interval of 11 days). Emissions originating from the other hemisphere are probably less visible or not visible at all due to radio beam oblateness and/or in/near-source refraction effects. Simulated radio arcs

match the observations, within 1–2 h in time and a few MHz in frequency. The observed thickness of the arcs is consistent with a cone wall thickness ~1°. The unique geometry of the Juno orbit allows Juno to observe Io-DAM arcs with a shape different from that usually observed from the Earth. The longer duration and broader phase intervals covered by many arcs observed by Juno suggest that the absence of Io-Jupiter emission at Io phases close to ~180° as seen from Earth is a mere visibility effect. The predicted emission is actually observed only when the radio beaming angle $\theta = (k,B) \geq 70° \pm 5°$, providing new remote constraints on the generation of the decametric emission by the Cyclotron Maser Instability. These remote constraints will be compared to those provided by in situ particle measurements [*Louarn et al*., 2017], which will help to simulate non-Io emissions in future work. Comparison to ground-based decametric observations confirms the identification of Io arcs via ExPRES simulations and based on the time delay between observations of the same arc by Juno and from the Earth. It also shows that Io-Jupiter emission is essentially permanent. By contrast with the situation near the equator, radio emissions observed from high magnetic latitudes around periJove #1 are likely mostly associated with the main auroral oval.

These results obtained for the Io-Jupiter emission suggest that we are reaching a good understanding of the radio emission generation. They also provide us directions for further improvements of ExPRES: (i) using optical images of aurorae to constrain the instantaneous position of the AFT footprints (instead of an average sine variation of the lead angle) and of hot spots along the auroral oval for identifying instantaneously active field lines hosting radio sources, (ii) using an updated internal magnetic field model, and (iii) incorporating beam oblateness and in/near-source refraction effects, we should achieve a better fitting of individual Io and non-Io radio arcs, eliminate or reduce the uncertainty of its predictions (~1–2 h and a few MHz), and thus derive accurate beaming angles and in turn assess the CMI-unstable electrons. Performing quantitative parametric fittings at various distances from the sources and comparing the results with in situ waves, magnetic field, and particle measurements (using Waves, MAG, and JADE experiments, respectively) will enable us to determine the intrinsic radio beaming angle at the source and its evolution (with refraction) toward the apparent radio beaming angle far from the source. This will also allow us to distinguish between a shell-driven emission refracted at oblique angles and a loss cone-driven emission.

The combination of Juno/Waves observations, ExPRES simulations, and Earth-based radio observations should similarly allow us to identify radio emission induced by the other Galilean satellites. Finally, when combined together, ground-based observations from the world-wide Juno.Ground.Radio collaboration will provide a quasi-continuous time coverage, enabling the identification of individual arcs and the investigation of the time variability of Jupiter's decametric emissions stereoscopically observed from Juno and the Earth, high-resolution dynamic spectra from, e.g., the NDA, and a flux calibration reference for Juno/Waves data [*Zarka et al*., 2004].

Acknowledgments
The authors thank the Juno mission team, especially the staff of the Juno Waves instrument, the CNES (Centre National d'Etudes Spatiales), the CNRS (Centre National de la Recherche Scientifique), the LESIA Wind/WAVES team, and the CDPP (Centre de Données de la Physique des Plasmas) for the provision of the Wind/WAVES data. The NDA, ExPRES, and Wind/Waves data used in this paper are reachable from the MASER (Measuring, Analysing and Simulating Emissions in Radio frequencies) website (http://maser.lesia.obspm.fr/), under the Data Access section. The Juno/Waves data used in this paper are reachable from the Planetary Data System (PDS) at http://pds.nasa.gov/. The research at the University of Iowa was supported by NASA through contract 699041X with the Southwest Research Institute. This work has been done within the LABEX Plas@par project and received financial state aid managed by the Agence Nationale de la Recherche, as part of the program "Investissements d'Avenir" under the reference ANR-11-IDEX-0004-02.

References

Allegrini, F., et al. (2017), Electron beams and loss cones in the auroral regions of Jupiter, *Geophys. Res. Lett.*, *44*, 7131–7139, doi:10.1002/2017GL073180.

Bagenal, F. (1994), Empirical model of the Io plasma torus: Voyager measurements, *J. Geophys. Res.*, *99*, 11,043–11,062, doi:10.1029/93JA02908.

Bagenal, F., et al. (2014), Magnetospheric science objectives of the Juno mission, *Space Sci. Rev.*, doi:10.1007/s11214-014-0036-8.

Bonfond, B., D. Grodent, J.-C. Gérard, A. Radioti, J. Saur, and S. Jacobsen (2008), UV Io footprint leading spot: A key feature for understanding the UV Io footprint multiplicity?, *Geophys. Res. Lett.*, *35*, L05107, doi:10.1029/2007GL032418.

Bougeret, J.-L., et al. (1995), WAVES: The radio and plasma wave investigation on the WIND spacecraft, *Space Sci. Rev.*, *71*, 231–265.

Carr, T. D., M. D. Desch, and J. K. Alexander (1983), Phenomenology of magnetospheric radio emissions, in *Physics of the Jovian Magnetosphere*, *Cambridge Planet. Sci. Ser.*, vol. 3, edited by A. J. Dessler, pp. 226–284, Cambridge Univ. Press, New York.

Cecconi, B., et al. (2012), Natural radio emission of Jupiter as interferences for radar investigations of the icy satellites of Jupiter, *Planet. Space Sci.*, *61*, 32–45.

Cecconi, B., et al. (2017), *JUNO-Ground-Radio Observation Support*, *Planetary Radio Emissions VIII*, edited by G. Fischer et al., Austrian Acad. Press, Vienna.

Faden, J., R. S. Weigel, J. Merka, and R. H. W. Friedel (2010), Autoplot: A browser for scientific data on the web, *Earth Sci. Inform.*, *3*, 41–49, doi:10.1007/s12145-010-0049-0.

Galopeau, P. H. M., and M. Y. Boudjada (2016), An oblate beaming cone for Io-controlled Jovian decameter emission, *J. Geophys. Res. Space Physics*, *121*, 3120–3138, doi:10.1002/2015JA021038.

Hess, S., B. Cecconi, and P. Zarka (2008a), Modeling of Io-Jupiter decameter arcs, emission beaming and energy source, *Geophys. Res. Lett.*, *35*, L13107, doi:10.1029/2008GL033656.

Hess, S., F. Mottez, P. Zarka, and T. Chust (2008b), Generation of the Jovian radio decametric arcs from the Io flux tube, *J. Geophys. Res.*, *113*, A03209, doi:10.1029/2007JA012745.

Hess, S. L. G. and P. Zarka (2011), Modeling the radio signature of the orbital parameters, rotation, and magnetic field of exoplanets, *Astron. Astrophys.*, *531*, A29, 9,

Hess, S. L. G., B. Bonfond, P. Zarka, and D. Grodent (2011), Model of the Jovian magnetic field topology constrained by the Io auroral emissions, *J. Geophys. Res.*, *116*, A05217, doi:10.1029/2010JA016262.

Hess, S. L. G., et al. (2017), *ISaAC Model*, *Planetary Radio Emissions VIII*, edited by G. Fischer et al., Austrian Acad. Press, Vienna.

Hinson, D. P., J. D. Twicken, and E. T. Karayel (1998), Jupiter's ionosphere: New results from Voyager 2 radio occultation measurements, *J. Geophys. Res.*, *103*, 9505–9520, doi:10.1029/97JA03689.

Kaiser, M. L., P. Zarka, W. S. Kurth, G. B. Hospodarsky, and D. A. Gurnett (2000), Cassini and Wind stereoscopic observations of Jovian nonthermal radio emissions: Measurement of beam widths, *J. Geophys. Res.*, *105*, 16,053–16,062, doi:10.1029/1999JA000414.

Kurth, W. S., et al. (2017), A new view of Jupiter's auroral radio spectrum, *Geophys. Res. Lett.*, *44*, 7114–7121, doi:10.1002/2017GL072889.

Lamy, L., P. Zarka, B. Cecconi, S. Hess, and R. Prangé (2008), Modeling of Saturn kilometric radiation arcs and equatorial shadow zone, *J. Geophys. Res.*, *113*, A10213, doi:10.1029/2008JA013464.

Lamy, L., B. Cecconi, P. Zarka, P. Canu, P. Schippers, W. S. Kurth, R. L. Mutel, D. A. Gurnett, J. D. Menietti, and P. Louarn (2011), Emission and propagation of Saturn kilometric radiation: Magneto-ionic modes, beaming pattern and polarization state, *J. Geophys. Res.*, *116*, A04212, doi:10.1029/2010JA016195.

Lamy, L., R. Prangé, W. Pryor, J. Gustin, S. V. Badman, H. Melin, T. Stallard, D. G. Mitchell, and P. C. Brandt (2013), Multispectral simultaneous diagnosis of Saturn's aurorae throughout a planetary rotation, *J. Geophys. Res. Space Physics*, *118*, 4817–4843, doi:10.1002/jgra.50404.

Lamy, L., P. Zarka, B. Cecconi, L. Klein, S. Masson, L. Denis, A. Coffre, and C. Viou (2017), 1977–2017: 40 years of Decametric observations of Jupiter and the Sun with the Nancay Decameter Array, Planetary Radio Emissions VIII, edited by G. Fischer et al., Austrian Acad. Press, Vienna.

Louarn, P., et al. (2017), Generation of the Jovian hectometric radiation: First lessons from Juno, *Geophys. Res. Lett.*, *44*, 4439–4446, doi:10.1002/2017GL072923.

Louis, C. K., L. Lamy, P. Zarka, B. Cecconi, and S. Hess (2017), Detection of Jupiter decametric emissions controlled by Europa and Ganymede with Voyager/PRA and Cassini/RPWS, *J. Geophys. Res. Space Physics*, doi:10.1002/2016JA023779, in press.

Marques, M. S., P. Zarka, E. Echer, V. B. Ryabov, M. V. Alves, L. Denis, and A. Coffre (2017), Statistical analysis of 26 years of observations of decametric radio emissions from Jupiter, *Astron. Astrophys.*, doi:10.1051/0004-6361/201630025.

McComas, D. J., et al. (2013), The Jovian Auroral Distributions Experiment (JADE) on the Juno mission to Jupiter, *Space Sci. Rev.*, 1–97, doi:10.1007/s11214-013-9990-9.

Mottez, F., S. L. G. Hess, and P. Zarka (2010), Explanation of dominant oblique radio emission at Jupiter and comparison to the terrestrial case, *Planet. Space Sci.*, *58*, 1414–1422.

Mutel, R. L., I. W. Christopher, and J. S. Pickett (2008), Cluster multispacecraft determination of AKR angular beaming, *Geophys. Res. Lett.*, *35*, L07104, doi:10.1029/2008GL033377.

Queinnec, J., and P. Zarka (1998), Io-controlled decameter arcs and Io-Jupiter interaction, *J. Geophys. Res.*, *103*, 26,649–26,666, doi:10.1029/98JA02435.

Zarka, P. (1998), Auroral radio emissions at the outer planets: Observations and theories, *J. Geophys. Res.*, *103*, 20,159–20,194, doi:10.1029/98JE01323.

Zarka, P. (2004), Fast radio imaging of Jupiter's magnetosphere at low frequencies with LOFAR, *Planet. Space Sci.*, *52*, 1455–1467.

Zarka, P., B. Cecconi, and W. S. Kurth (2004), Jupiter's low frequency radio spectrum from Cassini/RPWS absolute flux density measurements, *J. Geophys. Res.*, *109*, A09S15, doi:10.1029/2003JA010260.